Characterization of Porous Thin Films Using Quartz Crystal Shear Resonators

R. Etchenique*,†,‡ and V. L. Brudny§,||

Centro de Investigaciones Químicas, Universidad Autónoma del Estado de Morelos, Av. Universidad No. 1001 Col. Chamilpa, CP 62210, Cuernavaca, Morelos, México, and Facultad de Ciencias, Universidad Autónoma del Estado de Morelos, Av. Universidad No. 1001 Col. Chamilpa, CP 62210, Cuernavaca, Morelos, México

Received August 25, 1999. In Final Form: December 14, 1999

A new model for the characterization of porous materials using quartz crystal impedance analysis is proposed. The model describes the equivalent electrical and/or mechanical impedance of the quartz crystal in contact with a finite layer of a rigid porous material which is immersed in a semi-infinite liquid. The characteristic porosity length (ξ), layer thickness (d), liquid density (ρ), and viscosity (η) are taken into account. For films thick compared with the characteristic porosity length ($d \gg \xi$), the model predicts a net increase of the area which is translated into a linear relationship between the quartz equivalent impedance $\mathbf{Z} = R + XL$ ($XL = i\omega L$, $\omega = 2\pi f$, f being the oscillation frequency of the quartz resonator) and the ratio d/ξ. For low-viscosity Newtonian liquids, for which the velocity decay length $\delta = (2\omega\eta/\rho)^{1/2}$ is much smaller than ξ, $\mathbf{Z}$ corresponds to the impedance of a semi-infinite liquid in contact with an increased effective quartz area which scales with the ratio d/ξ. In this case, $R = XL$ in agreement with Kanazawa equation. For liquids of higher viscosity, the effect of the fluid trapped by the porous matrix is apparent and is reflected in the impedance, which has an imaginary part (XL) higher than its real part (R). In the limit of a very viscous liquid, the movement of the porous film is completely transferred to the liquid and all the mass moves in-phase with the quartz crystal electrode. In this limiting case the model predicts a purely inductive impedance, which corresponds to a resonant frequency in agreement with the Sauerbrey equation. The model allows us, for the first time, to explain the almost linear behavior of R vs XL along the growth process of conducting polymers, which present a well-known open fibrous structure. Films of polyaniline−polystyrenesulfonate were deposited on the quartz crystal under several conditions to test the model, and a very good agreement was found.

Introduction

Shear mode quartz resonators are widely used to measure the viscoelastic properties of materials such as polymers,[1] molecular composites,[2] gels,[3] etc. As early as 1949, Mason et al.[4] used a cylindrical quartz crystal to probe the viscoelastic properties of polymer solutions. A decade later, Sauerbrey[5] described the general dependence of the resonance frequency of a quartz crystal resonator as a function of the deposited mass of a metal in a vacuum.

Despite the general opinion that a quartz crystal resonator could not oscillate if put in contact with a highly damped medium as a liquid, several works demonstrated that oscillations were possible even in viscous media.[6−9] The immediate application was the use of transverse shear mode devices as microgravimetric devices (Quartz Crystal Microbalances), capable of nanogram detection in mass changes of rigid materials.

When the surface film is not entirely rigid, the quartz crystal response depends not only on the mass but also on the viscoelastic properties of the attached layer.[10] Several theoretical approaches to the viscoelastic layer problem were made. Reed et al.[11] derived a relationship between the complex admittance of a coated quartz resonator and the mass, density, and complex shear modulus $\mathbf{G} = G' + iG''$ of the deposited material. Martin and Granstaff[12] reported a completely equivalent equation and extended the analytical results to a bilayer.

Some studies of rough surfaces in contact with liquids using a quartz crystal microbalance (QCM) have been performed,[13] and a model for rough films has been proposed by Daikhin and Urbakh.[14]

Johannsmann[15] studied polymer rheology by means of multiharmonic impedance analysis. Etchenique and Calvo applied impedance analysis to perform gravimetry beyond the Sauerbrey limit.[16]

The case of a porous material, however, has not been treated extensively. Porous growth of some materials while

* Corresponding author. E-mail: rober@q1.fcen.uba.ar. Tel: +52 7 3297020. Fax: +52 7 3297040.

† Centro de Investigaciones Químicas, Universidad Autónoma del Estado de Morelos.

‡ On leave from DQIAyQF, Facultad de Ciencias Exactas y Naturales, Pab. 2, Universidad de Buenos Aires, Ciudad Universitaria, CP 1428, Buenos Aires, Argentina.

§ Facultad de Ciencias, Universidad Autónoma del Estado de Morelos.

|| On leave from Departamento de Física, Facultad de Ciencias Exactas y Naturales, Pab 1, Universidad de Buenos Aires, Ciudad Universitaria, CP 1428, Buenos Aires, Argentina.

(1) Noel, M. A.; Topart, P. A. *Anal. Chem*. **1994**, *66*, 484.
(2) Muramatsu, H.; Kimura, K. *Anal. Chem*. **1992**, *64*, 2502.
(3) Etchenique, R. A.; Calvo, E. J. *Anal. Chem*. **1997**, *69 23*, 4833.
(4) Mason, W. P.; Baker, W.; McSkimin, H. J.; Heiss, J. H. *Phys. Rev*. **1949**, *75*, *6*, 936.
(5) Sauerbrey, G.; *Z. Phys*. **1959**, *155*, 206.
(6) Nomura, T.; Minemura, A. *Nippon Kagaku Kaishi* **1980**, 1621.
(7) Konash, P. L.; Bastiaans, G. J. *Anal. Chem*. **1980**, *52*, 1929.
(8) Bruckenstein, S.; Shay, M. *J. Electroanal. Chem*. **1985**, *188*, 131.
(9) Kanazawa, K. K.; Gordon, J. G. *Anal. Chim. Acta* **1985**, *175*, 99.
(10) Martin, J.; Granstaff, V. E.; Frye, G. C. *Anal. Chem*. **1991**, *63*, 2272.
(11) Reed, C. E.; Kanazawa, K. K.; Kaufman, J. H. *J. Appl. Phys*. **1990**, *68*, 1993.
(12) Granstaff, E.; Martin, S. J. *J. Appl. Phys*. **1994**, *75*, 1319.
(13) Liess, H.−D.; Knezevic, A. Rother, A.; Muenz, J. *Faraday Discuss*. **1997**, *107*, 39.
(14) Daikhin, L.; Urbakh, M. *Langmuir* **1996**, *12*, 6354.
(15) Wolff, O.; Seydel, E.; Johannsmann, D. *Faraday Discuss*. **1997**, *107*, 91.
(16) Etchenique, R. A.; Calvo, E. J. *Electrochem. Commun*. **1999**, *1* (5), 167.

10.1021/la991145q CCC: $19.00
Published on Web 04/21/2000

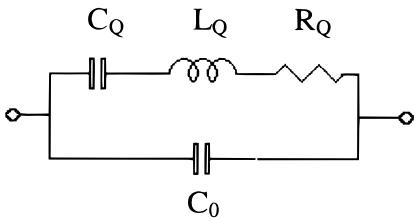

Figure 1. BVD equivalent circuit of a quartz crystal resonator.

monitored by QCM has been reported,[17] but the QCM is used only to measure the mass changes using the Sauerbey equation.

Porous materials have properties which make them very useful for a wide field of applications. The main property of any porous film is its very high area as compared with a solid deposit. Porous materials are therefore widely use in catalysis, batteries, supercapacitors, and other applications where the area plays an important role.

Conducting polymers (polyaniline, polypyrrole, polythiophene, etc.) have been widely studied due to their numerous practical applications. Many of them show very high capacitive characteristics,[17] a very fast switch between their conducting and insulating states,[18] high physical and chemical stability,[18] and also electrochromism.[19] The growth of conducting polymer films can be performed in several ways, either chemical or electrochemical. Electropolymerization of anilines, thiophenes, pyrroles, etc. often produces very fibrous and porous structures which have been very well characterized by scanning electron microscopy.[17]

Growth and electrochemical properties of several conducting polymers have often been measured by means of QCM. Noel and Topart[20] reported in situ monitoring of viscoelastic and mass changes during electrochemical growth and redox switching of poly(pyrrole). In most cases, however, the porosity of the film under study is not taken into account in the quartz impedance analysis. Hillman et al.[21] have reported the quartz impedance analysis of poly(2,2-bithiophene) but performed on the basis of a smooth viscoelastic material. Neglecting the effect of the porosity, however, might yield misleading results, as was previously shown.[22]

In this paper we propose a new model that permits the analysis of the quartz impedance parameters when a porous film is attached to the quartz resonator, in contact with a liquid phase. This approach neglects the viscoelastic properties of the porous film; therefore it can only be applied to rigid films. We also apply the proposed model to the analysis of the electrodeposition of polyaniline−polystyrenesulfonate films.

Quartz Resonator Impedance

The mechanical properties of the quartz resonator can be described in terms of an electrical equivalent circuit. Figure 1 shows the widely used Butterworth−Van Dyke (BVD) model,[23] in which the inertial mass of the quartz is represented by the inductance L_Q, the quartz compliance by the capacitance C_Q, and the mechanical damping by the resistance R_Q. These three equivalent components describe the motional branch of the equivalent circuit. An additional capacitance C_0 represents the parasitic electrical capacitance of the wires, connections, holder, and the quartz crystal itself and has no mechanical equivalence.

When nonpiezoelectric layers are attached to the quartz resonator, the equivalent parameters change. We define the equivalent electrical impedance of the bare quartz resonator as $\mathbf{Z}_Q = R_Q + i\omega L_Q = R_Q + XL_Q$. If the impedance of the quartz resonator $\mathbf{Z}_Q$ is very high compared with the nonpiezoelectric layer impedance $\mathbf{Z}_f = R_f + XL_f$, the total electrical equivalent impedance of the system can be approximated as $\mathbf{Z} = \mathbf{Z}_Q + \mathbf{Z}_f$.[10]

Martin and Granstaff[12] have derived an expression for the electrical equivalent impedance $\mathbf{Z}$ in terms of the mechanical impedance $\mathbf{Z}_M$

$$\mathbf{Z} = \frac{2\omega L_Q}{\pi(\mu_Q \rho_Q)^{1/2}} \mathbf{Z}_M \tag{1}$$

with

$$L_Q = \frac{h_Q^3 \rho_Q}{8Ae_{26}^2}$$

where $\mu_Q = 2.957 \times 10^{10}$ N m^{-2} is the elastic constant for piezoelectrically stiffened quartz, $\rho_Q = 2650$ kg m^{-3} is the density of the quartz, h_Q is the thickness of the quartz, A is the active area of the gold electrode, and $e_{26} = 9.652 \times 10^{-2}$ C m^{-2} is the quartz piezoelectric stress constant.

Porous Nonpiezoelectric Layer Model

The description of the flow of an incompressible, viscous fluid through porous media is a complex problem. If low Reynold numbers and nonslip boundary condition at the solid−liquid interfaces are assumed, and for a characteristic size of the porosity less than the thickness of the fluid layer, Darcy's law is often used[24,25]

$$U = -\frac{\xi^2}{\eta} \nabla p \tag{2}$$

where U is the average velocity, p is the pressure, η is the fluid viscosity, and ξ^2 is the permeability of the porous media. This quantity, ξ^2, depends on the random microstructure and can only be predicted by approximate theories;[25] its square root ξ is the characteristic length of the porosity.[14]

The system we would like to model is depicted in Figure 3. It consists of a layer of porous material of thickness d, rigidly attached to a flat quartz crystal oscillator. The porous layer is filled with a liquid of density ρ and viscosity η. The liquid phase occupies a region much larger than d and can be considered as a semi-infinite layer. We consider that the fluid moves as a laminar flow, where the velocity is parallel to the plane of the quartz crystal (x direction). Only variations of the relevant quantities along a direction perpendicular to the velocity (z direction) are considered. The quartz crystal (and therefore the porous layer) oscillates with frequency ω and drives the motion of the liquid.

On the basis of Darcy's law, Brinkman[26] derived an equation that intends to describe the flow through a porous

(17) Ferraris, J. P.; Eissa, M. M.; Brotherston, I. D.; Loveday, D. C.; Moxey, A. A. *J. Electroanal. Chem.* **1998**, *459*, 131, 57.
(18) Dinh, H. N.; Ding, J.; Xia, S. J.; Birss, V. I. *J. Electroanal. Chem.* **1998**, *459*, 131, 45.
(19) DuBois, C. J., Jr.; McCarley, R. L. *J. Electroanal. Chem.* **1998**, *454*, 99.
(20) Topart, P. A.; Noël, M. A. *Anal. Chem.* **1994**, *66*, 2926.
(21) Bandey, H. L.; Hillman, A. R.; Brown, M. J.; Martin, S. J. *Faraday Discuss.* **1997**, *107*, 105.
(22) Etchenique, R.; Brudny, V. L. *Electrochem. Commun.* **1999**, *1*, 441.
(23) Van Dyke, K. *Phys. Rev.* **1925**, *25*, 895.
(24) Sahimi, M. *M. Rev. Modern Phys.* **1993**, *65*, 1393.
(25) Rubinstein, J.; Torquato, S. *J. Fluid Mech.* **1989**, *206*, 25.
(26) Brinkman, H. C. *Appl. Sci. Res., A* **1947**, *1*, 27.

layer. In Brinkman's equation the effect of the solid phase on the liquid flow is given by a resistive force that has the form $F_r = \eta\xi^{-2}(v_o - v)$, where ξ is the characteristic length of porosity, $v = v(z)$ is the fluid velocity, and v_0 is the amplitude of the driving velocity, which oscillates with frequency ω.

Brinkman's equation was used by Daikhin and Urbakh[14] to model the effect of surface roughness and morphology of nonuniform surface films on a QCM response in liquids.

However, no attempts have been made, to our knowledge, to model the response of the QCM to a porous material in this way.

When the excitation frequency is small, the viscosity is high, or the permeability is low, the velocity decay length $\delta = (2\eta/\omega\rho)^{1/2}$ can be much greater than the porosity characteristic length ξ, and Brinkman's equation may be applied. In this case, the liquid moves *in phase* with the applied force given by the solid matrix. Therefore, for a real value of the force, the velocity is also real.

For higher frequencies, high permeabilities, or low liquid viscosities, when $\delta \sim \xi$, the regime changes from viscous to inertial[24,27] and the permeability coefficient is no longer a real number but a complex quantity.[27−29] This means that the velocity of the liquid may now be a complex quantity even for a real value of the applied force. This merely means that the velocity is *out of phase* with the matrix movement. In the limit, when the porosity characteristic length ξ is much greater than the velocity decay length, the velocity wave induced by the movement of the porous matrix in any point of the liquid vanishes completely before it reaches another solid part. Therefore, any region of the liquid in contact with the porous structure can be considered as semi-infinite, and the system behaves as a bare resonator with its area increased due to the presence of the porous matrix.

We propose the use of a reactive force of the form

$$F_r = v_0 \frac{\eta}{\xi^2}\left(1 + \frac{i\omega\rho}{\eta}\xi^2\right)^{1/2} - v\frac{\eta}{\xi^2}\left(1 + \frac{i\omega\rho}{\eta}\xi^2\right)^{1/2} \quad (3)$$

We use the term "reactive" force instead of "resistive" force to enphasise the complex nature of the proportionality between the velocity and the applied force.

The first term in eq 3 represents the excitation of the liquid by the porous matrix, which oscillates with velocity v_0. The complex permeability is given by $\xi^2/(1 + i\omega\rho\xi^2/\eta)^{1/2}$. For high viscosities or small pores, the permeability tends to ξ^2 and the real limit (Brinkman's equation) is recovered. For low viscosities or big pores, this term scales as ξ/δ and its complex phase is $\pi/2$, as expected for the movement of a semi-infinite layer of liquid.

The second term represents the damping of the liquid velocities by the matrix. For low viscosities or big pores, the velocity in the liquid phase is much smaller than the matrix velocity while for high viscosities or small pores, the complete form tends to Brinkman's equation. We have chosen to use the real coefficient ξ^2 as an approximation for the complex permeability in the second term of eq 3. This approximation yields small errors and allows us to obtain a simple physical interpretation of the final form of the acoustical impedance. The fluid velocity then obeys the following equation for $0 < z < d$:

$$i\omega\rho v = \eta\frac{\partial^2 v}{\partial z^2} + v_0\frac{\eta}{\xi^2}\left(1 + \frac{i\omega\rho}{\eta}\xi^2\right)^{1/2} - v\frac{\eta}{\xi^2} \quad (4)$$

For $z > d$ it behaves according to the following equation:

$$i\omega\rho v = \eta\frac{\partial^2 v}{\partial z^2} \quad (5)$$

The fluid velocity should also fulfill the nonslip boundary condition at the fluid−quartz crystal interface and the continuity conditions for velocity and stresses at $z = d$, namely

$$v(z{=}0,t) = v_0\exp(i\omega t) \quad (6)$$

$$v(z{=}d^+) = v(z{=}d^-) \quad (7)$$

$$\frac{\partial v}{\partial z}(z{=}d^+) = \frac{\partial v}{\partial z}(z{=}d^-) \quad (8)$$

The solution of eqs 4 and 5 subject to boundary conditions eqs 6 to 8 is

$$v(z) = C_0 + C_1\exp(kz) + C_2\exp(-kz) \quad (9)$$

$$0 < z < d$$

$$v(z) = A\exp(ik_0 z) \quad (10)$$

$$z > d$$

with

$$k_0 = (i\omega\pi/\eta)^{1/2}$$

$$k = (k_0^2 + \xi^{-2})^{1/2}$$

$$C_0 = 1/\xi k$$

$$C_1 = \frac{v_0}{2W}\left[(k - k_0)\exp(-kd)\left(1 - \frac{1}{\xi k}\right) - \frac{k_0}{\xi k}\right]$$

$$C_2 = \frac{v_0}{2W}\left[(k + k_0)\exp(kd)\left(1 - \frac{1}{\xi k}\right) + \frac{k_0}{\xi k}\right]$$

$$W = k_0\sinh(kd) + k\cosh(kd)$$

$$A = \frac{k(2C_1\exp(kd) + C_0)}{(k - k_0)\exp(-k_0 d)}$$

The mechanical impedance of the liquid film is defined as the ratio of the force applied on the liquid to the velocity. Since in our case the force that drives the motion is applied not only by the quartz crystal in contact with the liquid but also by the porous matrix, the way to compute it is to integrate this force per unit volume, that is

$$Z_{Mf} = \frac{1}{v_0} i\omega\rho\int_0^\infty v(z)\,dz \quad (11)$$

with

$$\int_0^\infty v(z)\,dz = \frac{1}{k_0} + \frac{d}{\xi k} - \frac{1}{\xi W}\left[\frac{2k_0}{k^2}(\cosh(kd) - 1) + \frac{1}{k}\sinh(kd) + \frac{1}{k_0}(\cosh(kd) - 1)\left(\frac{1}{\xi k} - 1\right)\right]$$

(27) Charlaix, E.; Kushnick, A. P.; Stokes, J. P. *Phys. Rev. Lett.* **1988**, *61*, 14, 1595.
(28) Johnson, D. L.; Koplik, J.; Dashen, R. *J. Fluid Mech.* **1987**, *176*, 379.
(29) Knackstedt, M. A.; Sahimi, M.; Chan, D. Y. C. *Phys. Rev. E* **1993**, *47*, 4, 2593.

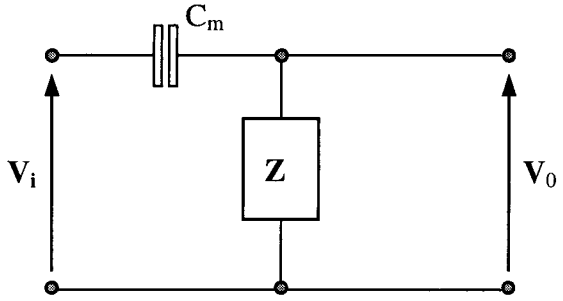

Figure 2. Transference voltage divider form by the measuring capacitance C_m and the quartz resonator impedance **Z**.

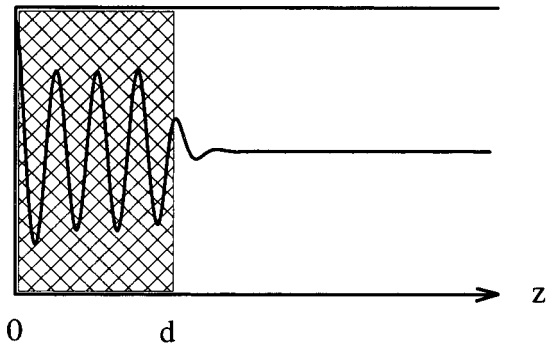

Figure 3. Schematic of the proposed model system. The *z* coordinate measures the distance from the quartz surface. The porous film (shaded) has a thickness *d*. The shear wavelength is not shown in the same scale.

Figure 4 shows the modulus of the mean velocity of the liquid near the quartz crystal for different porous film thicknesses *d*. In this simulation, the characteristic porosity length is kept constant, $\xi = 200$ nm, and the liquid density ρ and viscosity η are the corresponding parameters for water.

When no film is attached, the velocity profile is the one predicted for a smooth surface in contact with a Newtonian semi-infinite liquid[30] (Figure 4a). When the porous film grows, the profiles change, as expected since a significant part of the fluid is moved by the porous matrix (Figure 4b). For relatively thick films compared with ξ, the mean velocities in the bulk of the porous film remain constant (Figure 4c,d).

It is important to note that the calculated velocity for each value of *z* represents an average over the *x* and *y* directions. Local velocities inside the porous film can be very different than this average, specially near the matrix structure, where the fluid tends to move in-phase with the rigid porous film.

Figure 5 shows the velocity profiles for porous films of different porosity ξ immersed in water. Figure 5a corresponds to a very open porous structure ($\xi = 500$ nm). In this case, the porosity length is high compared with the velocity decay length in the liquid ($\delta \sim 200$ nm), and the liquid behaves as semi-infinite in nearly all of the porous matrix. The mean velocities in the bulk of the film (full line) are less than 0.25 times the matrix velocity. Far from the matrix structure the liquid is virtually static. The real and imaginary parts of the velocity (dots) are almost equal, as expected for a semi-infinite liquid. These components of the mean velocity lead to an impedance with equal resistive and inductive parts, which corresponds to the Kanazawa behavior.

As the porosity parameter ξ becomes smaller (Figure 5b), the mean velocity in the film increases and its real part (in-phase movement) is clearly higher than the imaginary part. For even smaller porosity lengths (Figure 5c), the mean velocity tends to the matrix velocity and the movement is mainly in-phase, a behavior that corresponds to a liquid rigidly "trapped" by the porous film. In this case, the impedance will have a purely inductive component, that shifts the resonant frequency as expected from the Sauerbrey equation.

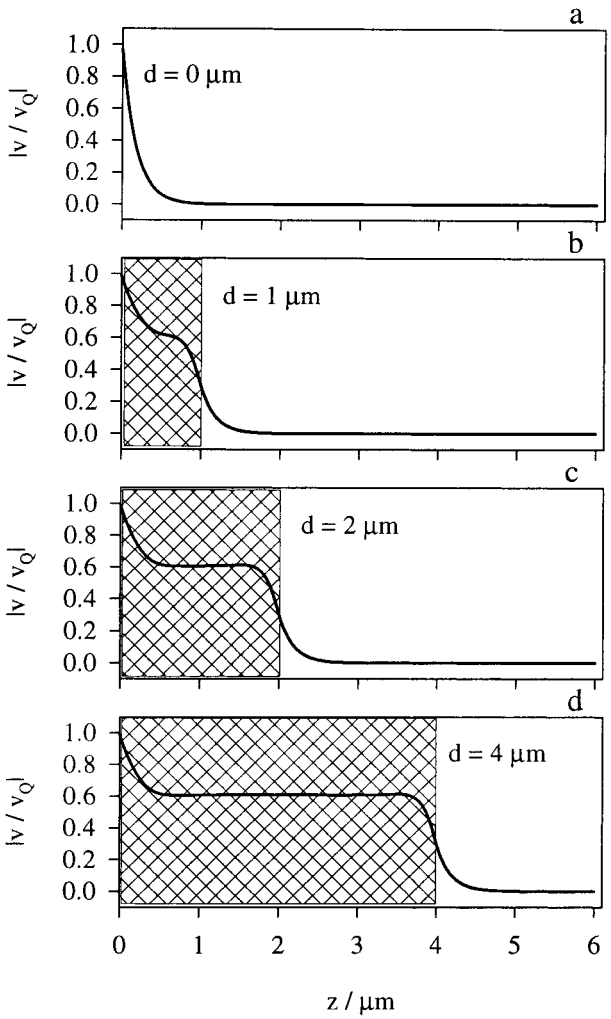

Figure 4. Velocity profiles in the liquid near the quartz surface for a bare crystal (a) and three different thickness of the attached porous material (b−d) of porosity length $\xi = 200$ nm immersed in water ($\rho = 1$ g·cm^{-3} and $\eta = 1$ cP).

Materials and Methods

All the measurements were performed using a QCM cell totally made of acrylic. The polished 14 mm gold-coated AT cut quartz crystals employed were purchased from ICM Company, Inc., Oklahoma City, OK. The crystals were mounted on the cell by means of sealing nitrile O-rings with only one face in contact with the liquid and/or polymer films. The active area of the gold electrodes was 0.196 cm^2 and the thickness of the quartz was 0.168 mm. The QCM setup has been described elsewhere.[31]

Polyaniline films were grown galvanostatically or potentiostatically with current limiting, at different current densities and/or electrode potentials from a solution containing 50 mM aniline, 6−10 g/L sodium polystyrenesulfonate (PSS), and 1 M H_2SO_4.

All potentials are quoted against a saturated calomel electrode (SCE). All chemicals used were analytical grade (Aldrich). All measurements were performed at room temperature (23 °C).

(30) Kanazawa, K. K. *Faraday Discuss.* **1997**, *107*, 77.

(31) Calvo, E. J.; Etchenique, R.; Bartlett, P. N. Singhal, K.; Santamaria, C.; *Faraday Discuss.* **1997**, *107*, 141.

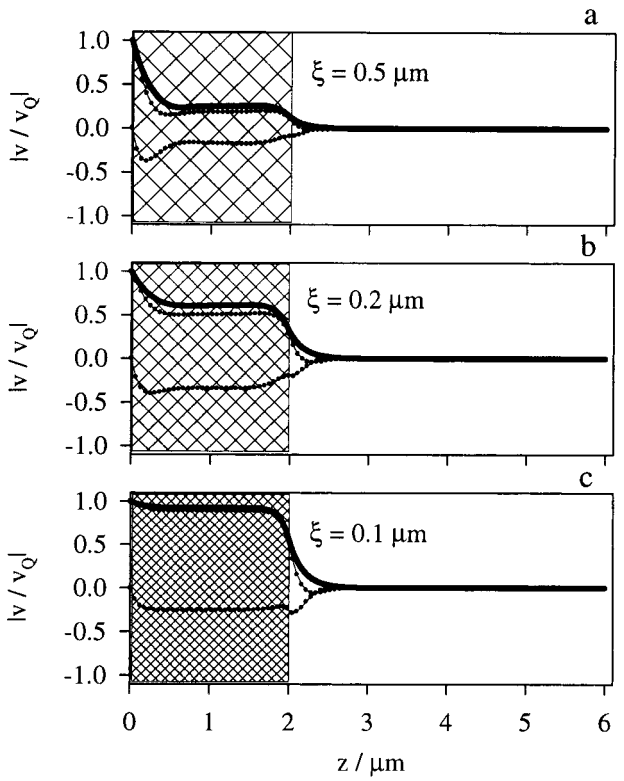

Figure 5. Velocity profiles (full line) in the liquid near the quartz surface for three porous layers of different porosity lengths: (a) $\xi = 500$ nm, (b) $\xi = 200$ nm, and (c) $\xi = 100$ nm. The dotted lines in each plot are the real (upper) and imaginary (lower) parts of the velocity.

Crystal Impedance Measurement

Several ways to measure the equivalent impedance que a quartz crystal resonator have been porposed. In this work, we use the transfer function method, which enables us to perform very fast measurement of both components of the impedance **Z**.

Figure 2 shows the measuring circuit consisting of an ac voltage divider formed by a quartz resonator impedance **Z** and the measuring capacitor C_m. A sinusoidal signal (10 mVpp) generated by a computer-controlled variable frequency oscillator (VFO) is applied to the input of the transference voltage divider.[32]

A sawtooth voltage was applied with a 12 bit digital-to-analog (D/A) converter attached to a 486 computer to the VFO to perform a linear frequency sweep. The sweep frequency limits were measured with an on-board frequencimeter also connected to the computer.

Both the input V_i and output V_o were amplified, rectified, and measured with a 12 bit A/D board attached to a 486 computer. The sample rate was 50 complete spectra per second, each containing 100 measured points.

The ratio of the output to input ac voltage for the transference voltage divider is

$$\frac{\mathbf{V_o}}{\mathbf{V_i}} = \left(1 + \frac{\mathbf{Z_m}}{\mathbf{Z}}\right)^{-1}$$

In terms of the BVD circuit, the modulus of the transfer function $|V_o/V_i|$ is given by

$$\left|\frac{V_o}{V_i}\right| = \frac{\left[\left(\omega L - \frac{1}{\omega C}\right)^2 + R^2\right]^{1/2}}{\left[\left(\omega L - \frac{1}{\omega C} + \frac{\omega L C_0}{\omega C C_m} - \frac{1}{\omega C_m}\right)^2 + \left(R + \frac{R C_0}{C_m}\right)^2\right]^{1/2}} \quad (12)$$

The BVD equivalent parameters R, L, and C_0 were obtained by least-squares fit of eq 12 to the measured data. The fitted values for $L = L_Q + L_f$ and $R = R_Q + R_f$ represent the total equivalent impedance of the covered quartz.

The contribution of the nonpiezoelectric porous film, R_f and L_f, can be obtained by subtraction of the parameters of the bare quartz. Since R_f and L_f are the impedance parameters of the film under study, in the next sections we will refer to them simply as R and L. The capacitance C represents the quartz crystal compliance and is not expected to vary in the experimental conditions. A fixed value of C was used according to the criterion proposed by Martin et al.[10]

Results and Discussion

To compare the theoretical and experimental results, we shall first analyze the predictions of our model for some relevant set of parameters.

Figure 6 shows the quartz equivalent impedance calculated for a growing film of constant $\xi = 200$ nm immersed in water. Although both of the components of the impedance, R and XL, show similar behaviors, a parametric plot of R vs XL shows that for thin films R is significantly lower than XL. For thick films compared with ξ, R is linear in XL. Note that in these calculations the porous matrix mass has been neglected. This mass, rigidly attached to the quartz crystal, introduces an additional contribution to XL that corresponds to the Sauerbrey shift of the film and can be easily obtained by measuring the dry film at the end of the experiment.

It is important to note that once the Sauerbrey mass of the film is subtracted, the slope of the R vs XL parametric plot in the linear region is directly related to the ratio ξ/δ. For high values of ξ, the slope of R vs XL tends to unity while for low ratios ξ/δ the slope tends to zero. Thus, if the viscosity of the liquid is known, the porosity length ξ can be easily obtained, as shown in Figure 7.

Figure 8 shows the passed charge and impedance parameters for the growth of a polyaniline−polystyrenesulfonate (PA−PSS) composite film. The PA−PSS film was grown potentiostatically, at 750 mV vs SCE, in a solution containing 1 M H_2SO_4, 50 mM aniline, and 10 g/L NaPSS with the maximum current limited to 80 μA. Before the potential was applied, $R \sim XL \sim 270 \pm 2\Omega$ as expected for a semi-infinite Newtonian liquid. Assuming density of 1 g·cm^{-3}, we calculate the viscosity of the solution to be $\eta = 1.6$ cP at 10 MHz.

The equivalent inductance (XL) follows the charge (q) curve. The shape of the equivalent resistance R is quite different and does not change until XL or q are greater than 30% of their maximum values. There are two major contributions to XL: the rigid mass of the film and the additional XL related to the interaction of the solution with the porous layer. The only contribution to R is the interaction between the solution and the porous film. Note that although there is also a surface contribution[14,33] to R and XL, it has been neglected here. This contribution is expected to be in the order of tens of ohms, while the

(32) Calvo, E. J.; Danilowicz, C.; Etchenique, R. *J. Chem. Soc., Faraday Trans.* **1995**, *91*, 4083.

(33) Beck, R.; Weil, K. *J. Electrochem. Soc.* **1992**, *139*, 453.

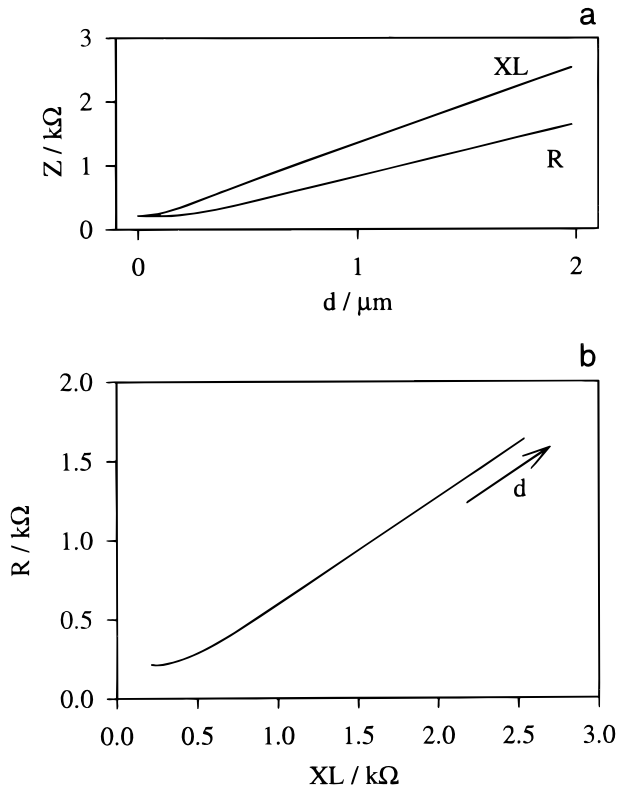

Figure 6. (a) Plot of the inductive (XL) and resistive (R) parts of the equivalent quartz impedance Z against the thickness for a porous film of $\xi = 200$ nm immersed in water. (b) Parametric polar plot of R against XL for the data in (a).

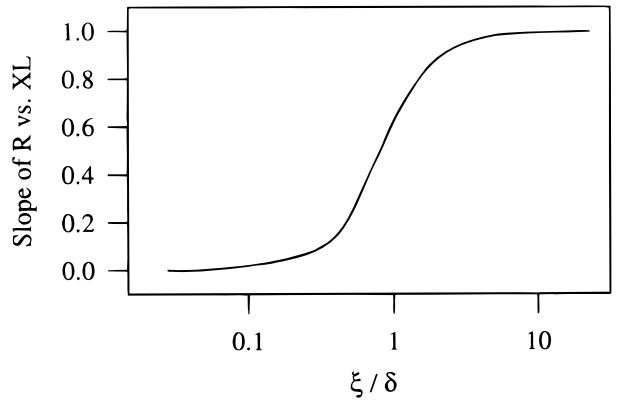

Figure 7. Plot of the slope of R against XL in the linear region of a parametric plot in function of the ξ/δ ratio. (ξ is the porosity length and δ is the velocity decay length.)

film mass and porous contribution for our films is in the range of the thousands of ohms.

With the grown film dried to constant weight in a nonhumid atmosphere, the Sauerbrey inductance XL_{dry} of PA−PSS in air was found to be 1114 Ω ($R_{dry} < 1$ Ω), which corresponds to a mass of 52.8 μg for the total mass of the porous structure and the layer of water molecules that is rigidly attached and cannot be expulsed at mild temperatures. Assuming that the deposited mass is proportional to the passed charge, the Sauerbrey inductance of the porous matrix can be calculated at any time as $XL_{mat}(t) = XL_{dry}q(t)/q_{max}$ and then subtracted from the measured inductive component.

The result of this calculation is shown in the parametric plot of Figure 9. The plot of the experimental values of R vs XL for the growth (dots) is in excellent agreement with the model calculations for $\eta = 1.6$ cP, $\rho = 1$ g·cm^{-3}, $\xi = 360$ nm, and $d = 1.51$ μm (solid line).

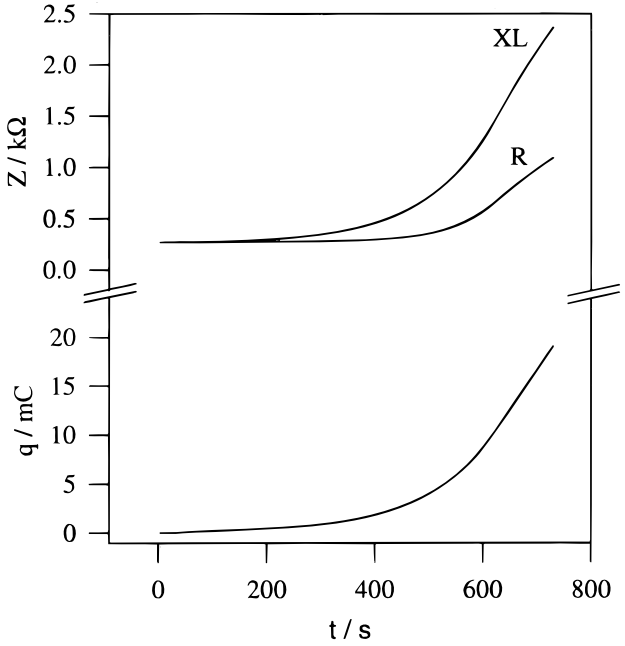

Figure 8. Impedance XL, resistance R, and charge q for the potentiostatic growth of a PA−PSS film. $E_{gr} = +750$ mV vs SCE in a solution containing 1 M H_2SO_4, 50 mM aniline, and 10 g/L NaPSS. Maximum current is limited to 80 μA.

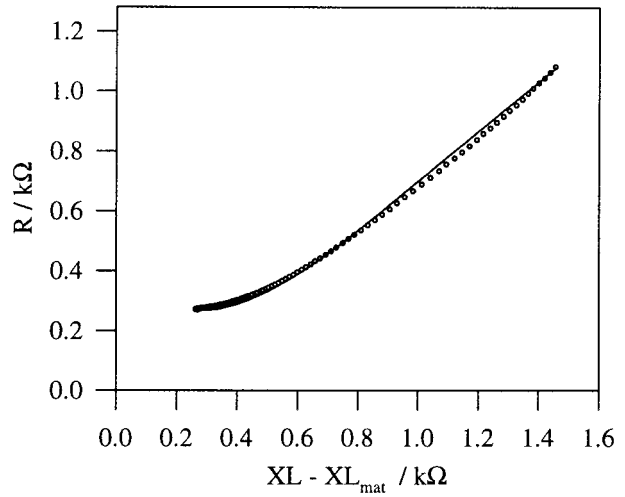

Figure 9. Parametric polar plot of the equivalent resistance R against the porous impedance XL (after subtraction of the Sauerbrey mass impedance XL_{mat}, see text) Open circles are experimental data, full line is the model for $\xi = 360$ nm and $d = 1.51$ μm. The solution viscosity $\eta = 1.6$ cP at 10 MHz was measured independently.

Measurement of surface roughness performed with atomic force microscopy (AFM) show structures with a root mean square (RMS) value of 400 ± 50 nm, which is in good agreement with the value $\xi = 360$ nm derived from our model. Note that only ξ and d were fitted using the model, while the density and the viscosity of the liquid are fixed data obtained independently.

Once the rigid mass contribution to XL is subtracted, the main variation of R and XL is due to the increase of effective area in contact with the liquid phase inside the porous matrix. Note that for a porous matrix of thickness d the area is expected to scale with the ratio (d/ξ). One of the effects of the porosity of the film, therefore, is simply

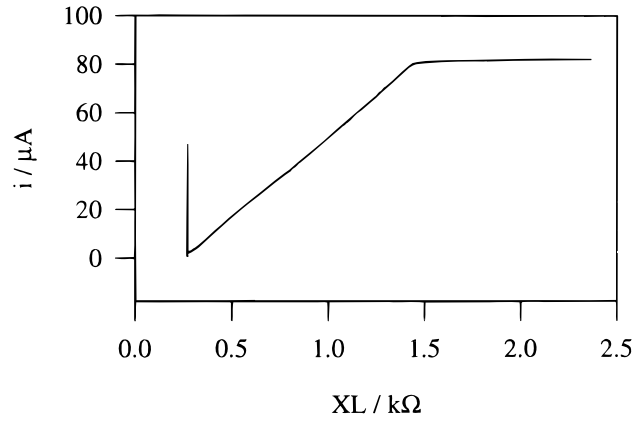

Figure 10. Plot of the faradaic current as function of the previously deposited polymer mass, represented by XL. Maximum current is limited to 80 μA. The spike corresponds to the initial transient of the chronoamperometry.

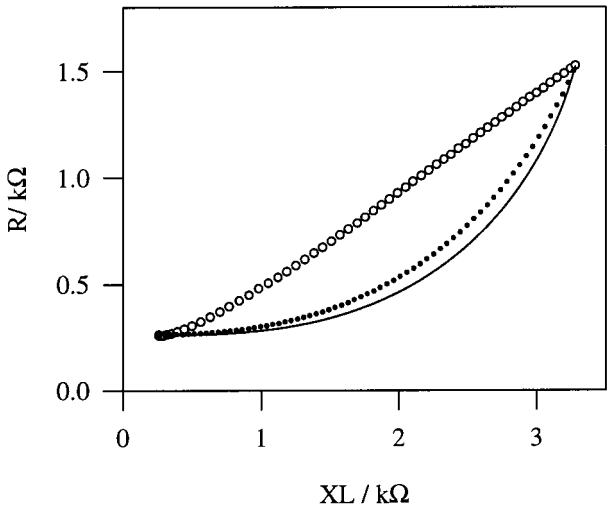

Figure 11. Open circles: Parametric plot for the galvanostatic growth of a PA−PSS film for current $i_{gr} = 27$ μA in 1 M H_2SO_4, 50 mM aniline, and 6 g/L NaPSS. Dots: Martin's model calculations for a viscoelastic layer of $G' = G'' = 4.77$ MPa ($\alpha = 1$) and $d_{max} = 1.195$ μm in contact with water. Full line: Same calculations for $G' \rightarrow 0$ and $G'' = 9.32$ MPa ($\alpha \rightarrow \infty$) and $d_{max} = 1.66$ μm.

to enhance the area of the polymer which can interact with the liquid and which can be affected by electrochemical processes.

Additional evidence about this area increase is shown in Figure 10. For the potentiostatic growth of PA−PSS, the current is proportional to *XL*, that is, to the previously deposited mass. Note that both the current and the charge follow the parameter *XL*. The plot of the charge (Figure 8) and the current vs time is exponential as expected for a film whose area is continuously increasing. When *XL* > 1.5 kΩ, the current is limited to 80 μA to prevent spurious reactions at high current densities. The spike at low *XL* values corresponds to the initial transient of the chronopotentiometry.

Deposition of PA−PSS in similar conditions is very reproducible. Galvanostatic PA−PSS deposition has also been performed, and the results obtained are close to the data already shown. Figure 11 shows a typical parametric plot for a galvanostatic deposition at constant current $i = 27$ μA from a solution containing 1 M H_2SO_4, 50 mM aniline, and 6 g/L NaPSS. Note the high similarities with the potentiostatically grown film, although this film can be grown much thicker than the former.

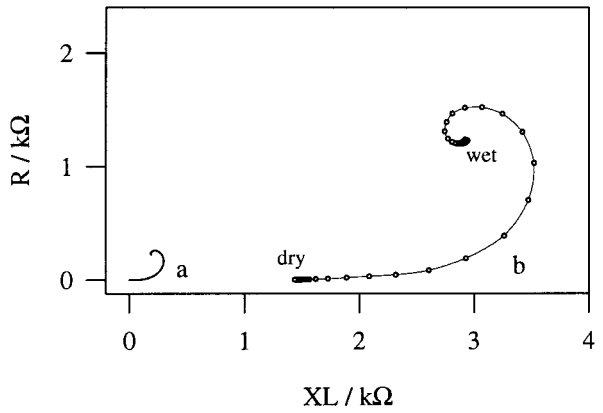

Figure 12. Polar parametric plot for the drying process of the galvanostatically grown film: open circles, experimental points; full line (a) calculations with Martin's model for a layer of water of decreasing thickness, (b) calculations with Martin's model and an enhanced area due to the porous matrix. Note that curve b is shifted to the right by aproximately 1.4 kΩ, which corresponds to the Sauerbrey mass of the dry porous film.

After a first upward curvature, the dependence of the resistance *R* on the inductance *XL* during deposition is linear (open circles). At the end of the deposition, $XL = 3291$ Ω, which corresponds to a resonant frequency shift of 34 921 Hz. If the film is assumed to be solid, rigid, and smooth, that value would correspond to a Sauerbrey mass of 155.9 μg. However, the high value of the equivalent resistance $R = 1530$ Ω shows that the Sauerbrey approximation is not valid.

If the film would be assumed to be viscoelastic, Martin's equation[12] could be used. In this case the impedance of a single viscoelastic layer covered by a viscous semi-infinite liquid can be described by

$$\mathbf{Z}_f = \frac{2\omega L_Q}{\pi(\rho_Q \mu_Q)^{1/2}} \left[\frac{(\rho_f \mathbf{G}_f)^{1/2} \tanh(i\omega d(\rho_f/\mathbf{G}_f)^{1/2}) + (\rho_1 \mathbf{G}_1)^{1/2}}{1 + ((\rho_1 \mathbf{G}_1)^{1/2}/(\rho_f \mathbf{G}_f)^{1/2}) \tanh(i\omega d(\rho_f/\mathbf{G}_f)^{1/2})} \right] \quad (13)$$

where $\mathbf{G}_l = iG''_l = i\omega\eta$ is the loss modulus of the liquid and ρ_l is the liquid density and $\mathbf{G}_f = G'_f + iG''_f$ is the complex mechanical modulus of the film and ρ_f is its density. The loss tangent $\alpha = G''_f/G'_f$ is widely used as an indication of the losses of a given material.[34] However, the values derived from eq 13 for the experimental initial and end points and a constant value of modulus $\mathbf{G}_f$ show a strong upward curvature for both $\alpha = 1$ (dots) and $\alpha \rightarrow \infty$ (full line) that do not correspond to the experimental data (open circles). It is possible to simulate the experimental data using eq 13 by assuming an ad-hoc variable $\mathbf{G}_f$ for each time of the deposition.[21] However, as only two independent parameters (*R* and *XL*) can be obtained with the impedance method,[35] this procedure can easily produce artifacts.

Once grown, this film was washed with distilled water several times and then the water was evaporated in a dry atmosphere. Figure 12b shows the drying process of the film. The transfer function method is fast enough to measure *R* and *XL* during the water evaporation.

The entire process takes about 1.5 s. Figure 12a shows the same drying process calculated from Martin's model[12]

(34) Ferry, J. D. *Viscoelastic Properties of Polymers*, 3rd ed.; Wiley: New York, 1980.

(35) Etchenique, R.; Weisz, A. D. *J. Appl. Phys.* **1999**, *86*, 4, 1994.

for a smooth film. Note that even though the shape of the experimental and theoretical curves is the same, the experimental values are several times higher that the theoretical ones. This is due to the enhancement of the effective area of the porous matrix. Also note that the experimental points are shifted by XL_{dry}.

The wet film presents a high value of R which corresponds to an almost semi-infinite liquid. This shows that this film presents quite an open structure. Calculations made with our model yield $\xi = 400$ nm, more than twice the decay length in pure water.

The observed behavior during drying indicates that the water far from the open porous structure evaporates faster that the water that is in close contact with the matrix. Less open films do not show this behavior, but rather an evaporation process that takes place in isolated zones which leads to a linear decrease of R and XL.

Conclusions

We have devised a new model for the analysis and characterization of rigid porous films that allows us to explain many well-known features of the QCM response to conducting polymer films growth. Linear plots of R vs XL for thick films and an upward curvature of R vs XL for thiner layers are predicted, in good agreement with the experimental results.

The parameters of the model are physically meaningful and permit the characterization of porous films, allowing the use of the quartz crystal microbalance in a field that is almost unexplored. The possibilities of fast and easy monitoring of porosity in the growth of porous layers opens new possibilities in the investigation of large area thin films, with applications in catalysts design, supercapacitors, battery electrodes, etc.

Three independent confirmations of the porosity of the PA−PSS films were shown: the AFM measurement, the linear relationship between deposition current, and deposited polymer mass and the drying process showing an area enhancement. Our model is in good agreement with the results obtained for these three experiments.

Further extensions of the model that take into account viscoelastic porous matrixes would be useful for the analysis of QCM impedance data obtained from complex systems, such as polymer−enzyme multilayers, DNA multilayers, PVF-coated electrodes, and other soft materials with large intrinsic area.

Acknowledgment. The authors wish to thank Erasmo Ovalle for the AFM measurements. This work was supported by Fundacion Antorchas and UBACYT. V. L. Brudny is a member of Carrera del Investigador, CONICET, Argentina.

LA991145Q